Journal of Chemistry and Allied Sciences
Volume 2, Issue 1 | 2026 | pp. 150–164
Original Research Article | ***Available online at*** **https://jcasjournal.org/**

AN OVERVIEW OF SOLID ELECTROLYTES FOR LITHIUM-ION BATTERIES BASED ON NASICON MATERIALS

Mohammed Isah Kimpa*[1,2], Sanda Abubakar Sadiq[1,3] Abubakar Sadiq Yusuf[1,5], Akoba Rashidah[2], Jibrin Alhaji Yabagi[3], Muhammad Bello Ladan[3], Abubakar Shehu Kollere[4], Ahmed Alhaji Abubakar[1], Haruna Isah[1,6], Fati Abdullahi[1], Muhammad Muhammad Ndamisto[7], Kasim Uthman Isah[1]

[1]Department of Physics, Federal University of Technology, P.M.B 65, Minna Nigeria.
[2]Department of Physics, Faculty of Science, Islamic University in Uganda, Mbale Campus.
[3]Department of Physics, Ibrahim Badamasi Babangida University, P.M.B 74, Lapai Nigeria.
[4]Trade Facilitation Division, Raw Material Research and Development Council, P.M.B 232, Abuja Nigeria
[5]Department of Physics and Astronomy, Auckland University of Technology, New Zealand.
[6]Department of Physics, Niger State Polytechnic, Zungeru Nigeria.
[7]Department of Chemistry, Federal University of Technology, P.M.B 65, Minna Nigeria.

Article History: Received May 2025; Revised June 2025; Accepted December 2025; Published online February 2026

***Correspondent Author**: Dr Mohammed Isah Kimpa (kimpa@futminna.edu.ng, mkimpa@iuiu.ac.ug;*
***ORCID**: https://orcid.org/0000-0003-0167-240X* ***Tel**: +2348038654849)*

Article Information

Citation: Kimpa, M. I., Sadiq, S. A., Yusuf, A. S., Rashidah, A., Yabagi, J. A., Ladan, M. B., Kollere, A. S., Abubakar, A. A., Isah, H., Abdullahi, F., Ndamisto, M. M., & Isah, K. U. (2026). An overview of solid electrolytes for lithium-ion batteries based on NASICON materials. Journal of Chemistry and Allied Sciences, 2(1), 150–164.
DOI: https://doi.org/10.60787/jcas.vol2no1.2

The Official Publication of the Tropical Research and Allied Network (TRANet), Department of Chemistry, *Federal University of Technology, Minna.*

Abstract

Lithium-ion solid electrolyte batteries have attracted great attention to replacing liquid electrolytes due to their cycling electrochemical properties, durable stability and safety. Numerous studies have been investigated to increase the performance of ionic-conductivity and enhance the stability of solid-state electrolytes, and its commercialization is broadly spread. This review article highlights the progress in developing NASICON-type solid electrolytes, which are made by solid-state reactions and wet-chemical procedures. Initially, researchers focused on the crystal structure, strength, and electrochemical properties of $LiZr_2(PO_4)_3$, but recent studies have shifted towards investigating the electrical conductivity, crystal structure and its compatibility with Li metal. Also, the indigenous research on $LiTi_2(PO_4)_3$ was pivoted on densification of the solid electrolyte to improve ionic conductivity by partial substitution of Ti^{4+} with Al^{3+} or B^{3+} now yields a promising ionic conductivity. $LiGe_2(PO4)_3$ is yet another Li-based NASICON electrolyte that, from the early stage, received extensive research majoring on the partial substitution of Al^{3+} with Ge^{4+} with the formula $Li_{1+x}Al_xGe_{2-x}(PO_4)_3$ to stabilize the crystal structure following experimental and computational analysis. Improved ionic conductivity currently increasing as a result of improved Li intensity affected by aliovalent Al^{3+} substitution. Numerous research efforts have been explored to improve the ionic conductivity and elevate the electrochemical and thermal stabilities of NASICON-type electrolytes. It deems it fit to bring forth a cascade of promising results that so far have been recorded in both the early and the current research efforts in improving the suitability of NASICON-type electrolytes.

***Keywords**: Failure rate, Markov Model, States, Mean Time to Failure, Repairable system.*

Graphical Abstract

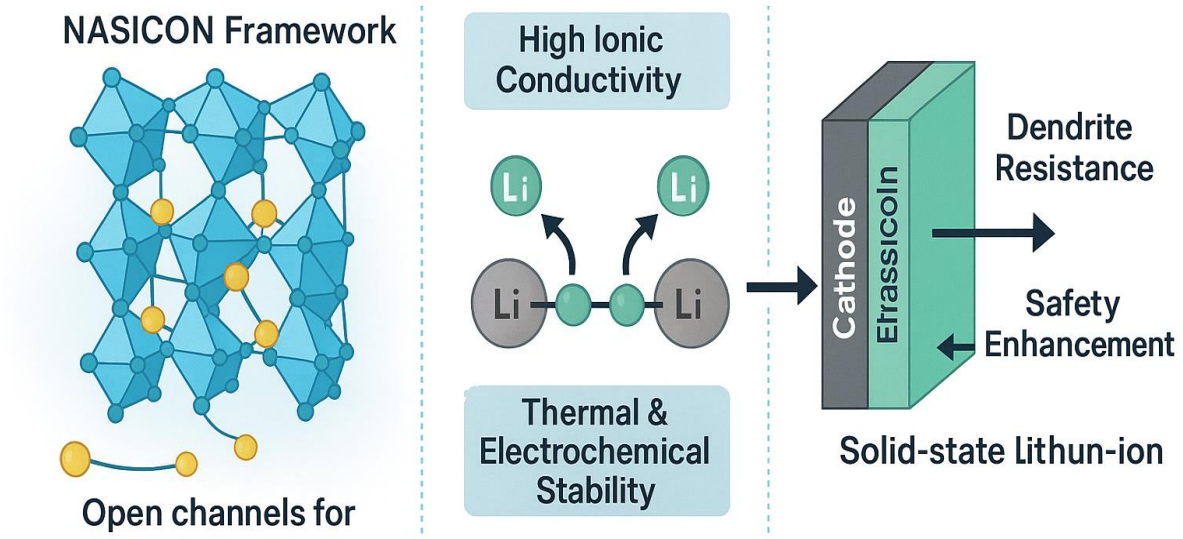

NASICON-type materials offer a promising path for safe, stable, and high-performance solid-state lithium-ion batteries due to their structural versatility and high Ionic conductivity.

1.0 INTRODUCTION

In response to growing global concerns over the environmental and sustainability impacts of fossil fuel consumption, significant efforts have been directed toward the development of clean and efficient energy conversion and storage technologies [1–9]. Lithium-ion batteries (LIBs) have emerged as the dominant energy storage solution for a wide range of applications, including portable electronic devices and electric vehicles, owing to their high energy and power densities [10–12].

Despite their widespread use, conventional lithium-ion batteries rely heavily on liquid electrolytes, which pose several safety challenges. These include risks of fluid leakage, flammability, and potential explosion. Moreover, the presence of organic solvents in liquid electrolytes contributes to degradation mechanisms that compromise the long-term performance and lifespan of the batteries [13–16].

Solid-state electrolytes (SSEs) offer a promising alternative to liquid electrolytes, particularly for applications demanding enhanced safety and performance over a wide temperature range [17,18]. As a core component of all-solid-state lithium batteries (ASSLBs), solid electrolytes must meet stringent requirements such as a wide electrochemical stability window, chemical compatibility with electrode materials, high ionic conductivity with minimal electronic conductivity, and cost-effective large-scale production [19]. Various types of solid electrolytes have been explored for lithium-ion systems, including NASICON-type, perovskite, polymer-based, sulfide-based, and garnet-type electrolytes [20]. Among these, NASICON-type (Na Super Ionic Conductor) solid electrolytes have shown particular promise due to their relatively high ionic conductivity, along with superior mechanical and thermal stability. These attributes make NASICON-type materials attractive candidates for next-generation solid-state battery technologies [21].

The synthesis of NASICON-type electrolytes has been accomplished using both solid-state reaction and wet-chemical methods [12]. Although the solid-state reaction method is well-established, it typically requires high processing temperatures (approximately 1200 °C) [22], extended synthesis durations (up to 24 hours), and suffers from unavoidable lithium loss during processing [23]. In contrast, wet-chemical approaches—such as co-precipitation, sol-gel, modified Pechini, and hydrothermal methods—enable better control at the molecular level, offer reduced synthesis temperatures, and produce uniformly reactive polycrystalline materials [24]. Owing to these advantages, wet-chemical methods are increasingly regarded as the most promising routes for the

  | DOI: https://doi.org/10.60787/jcas.vol2no1.2| CC BY 4.0

preparation of high-performance NASICON-type solid electrolytes [25]. This review focuses on recent advances in NASICON-type solid electrolytes, particularly in improving their ionic conductivity and electrochemical stability, with an emphasis on strategies to optimize their performance for use in lithium-ion battery systems.

2.0 NASICON type Electrolyte

The foundational work by Goodenough and co-workers in 1976 [26] introduced a novel class of sodium superionic conductor (NASICON) materials with the general formula $Na_{1+x}Zr_2P_{3-x}Si_xO_{12}$. More broadly, the NASICON framework is commonly represented as $AMM'(PO_4)_3$ or $AMM'P_3O_{12}$, where the structural versatility allows for extensive substitution at multiple crystallographic sites. In this structure, the A-site accommodates mobile cations, which may include a wide range of monovalent and multivalent ions such as alkali metals (Li^+, Na^+, K^+, Rb^+, Cs^+), alkaline earth metals (Mg^{2+}, Ca^{2+}, Sr^{2+}, Ba^{2+}), and other cations like H^+, H_3O^+, NH_4^+, Cu^+, Cu^{2+}, Ag^+, Pb^{2+}, Cd^{2+}, Mn^{2+}, Co^{2+}, Ni^{2+}, Zn^{2+}, Al^{3+}, rare earth cations (Ln^{3+}), Ge^{4+}, Zr^{4+}, and Hf^{4+}. In some cases, this site can also remain vacant, offering a high degree of configurational flexibility [10, 12, 27]. The M and M′ sites in the NASICON structure can be occupied by di-, tri-, tetra-, and penta-valent transition metal cations to maintain charge neutrality, including Zn^{2+}, Cd^{2+}, Ni^{2+}, Mn^{2+}, Co^{2+}, Fe^{3+}, Sc^{3+}, Ti^{3+}, V^{3+}, Cr^{3+}, Al^{3+}, In^{3+}, Ga^{3+}, Y^{3+}, Lu^{3+}, Ti^{4+}, Zr^{4+}, Hf^{4+}, Sn^{4+}, Si^{4+}, Ge^{4+}, V^{5+}, Nb^{5+}, Ta^{5+}, Sb^{5+}, and As^{5+}. Furthermore, the phosphorus (P) position within the phosphate tetrahedra may be partially substituted with silicon (Si), further enhancing the tunability of the structure.

This inherent flexibility allows for systematic manipulation of the A, M, M′, and P sites to engineer materials with tailored electrochemical properties, while preserving the fundamental topological identity of the NASICON framework. Despite the variety in elemental composition and mobile ions, all NASICON-based materials retain a common architectural motif that supports high ionic mobility [28]. These materials are crystalline and exhibit a rigid yet adaptable structure ideal for fast-ion conduction. For a crystalline solid electrolyte to function effectively, several key factors must be considered: the existence of continuous diffusion pathways within the lattice, a suitable match between the mobile ion radius and the channel size, sufficient sublattice disorder to facilitate ion hopping, and polarizable mobile cations in conjunction with a stable anionic substructure. Enhancing ionic conductivity hinges on the deliberate design and optimization of these structural attributes.

NASICON-type solid electrolytes are typically categorized into three primary families based on the choice of M-site cations: $LiZr_2(PO_4)_3$ (LZP), $LiTi_2(PO_4)_3$ (LTP), and $LiGe_2(PO_4)_3$ (LGP) [16]. Among various dopants explored, aluminum has emerged as the most effective substituent for significantly improving ionic conductivity, particularly in LTP and LGP systems, which show superior conductivities compared to LZP. With partial aluminum substitution, ionic conductivities exceeding 10^{-1} S cm^{-1} at room temperature have been reported. Nevertheless, grain boundary resistance remains a critical bottleneck that dictates the overall impedance of these materials, emphasizing the need for precise control over grain structure and morphology during synthesis and sintering [21].

Structurally, NASICON compounds most commonly crystallize in a rhombohedral lattice, corresponding to the space group $R\bar{3}c$. The structure comprises a three-dimensional network formed by corner-sharing PO_4 tetrahedra and MO_6 octahedra, creating interconnected channels that support lithium-ion diffusion. This arrangement offers structural robustness and compositional flexibility, which are vital for tuning the electrochemical properties of the material. Within the NASICON framework, lithium ions predominantly migrate through two distinct sites: M1 and M2. The M1 site, located at the Wyckoff position 6b (0, 0, 0) with site symmetry $\bar{3}$, lies between two MO_6 octahedra along the c-axis and is coordinated by six oxygen atoms. This site is energetically favored and typically exhibits the highest occupancy by lithium ions. The M2 site, positioned at Wyckoff 18e (x, 0, ¼) with site symmetry 2, is eightfold coordinated and situated between adjacent M1 sites. Each M1 site is flanked by six M2 sites, resulting in the M2 site having a multiplicity three times that of M1.

In stoichiometric $LiM_2(PO_4)_3$ compositions, lithium ions are generally confined to the M1 site. However, in $LiZr_2(PO_4)_3$, the introduction of trivalent metal dopants induces a structural distortion that shifts lithium occupancy from a simple octahedral site to a more distorted coordination environment. When trivalent cations are introduced according to the formula $Li_{1+x}M_x$^III M_{2-x}^IV$(PO_4)_3$, excess lithium tends to occupy additional interstitial sites beyond M1, initially presumed to correspond to the M2 position at Wyckoff 18e. However, given that the M2 cavity is larger than the ionic radius of Li^+, recent experimental and computational studies have revealed that lithium ions preferentially occupy newly identified positions. These findings suggest that the M2 site undergoes a spatial splitting, leading to the formation of the so-called M3 site, located at Wyckoff position 36f. The M3 site is

  DOI: https://doi.org/10.60787/jcas.vol2no1.2|

embedded within the original M2 cavity and offers a more energetically favorable environment for lithium ions, aligning with observed conductivity and structural behavior in many doped NASICON compositions [15].

2.1 $LiZr_2(PO_4)_3$

Prior to the year 2000, extensive foundational research had already been conducted on the crystal structure, thermal stability, and electrochemical behavior of $LiZr_2(PO_4)_3$, one of the earliest explored NASICON-type solid electrolytes [10]. It was observed that sintering $LiZr_2(PO_4)_3$ at elevated temperatures—typically around 1423 K—yielded a highly conductive rhombohedral phase with $R\bar{3}c$ symmetry, supporting ionic conductivities on the order of ~10^{-5} S cm^{-1}. In contrast, when sintered at lower temperatures, the material tended to crystallize into a mixture of monoclinic and triclinic phases. This phase coexistence markedly diminished the ionic conductivity, often to values around ~10^{-6} to 10^{-5} S cm^{-1}. Similar behavior was observed under low-temperature calcination conditions, where conductivity could drop even further—to as low as ~10^{-8} S cm^{-1}—indicating the critical role of high-temperature thermal treatment in achieving the desired crystalline phase and electrochemical performance [10].

To overcome these limitations and enhance the properties of $LiZr_2(PO_4)_3$, various substitution strategies have been explored. Partial replacement of Zr^{4+} with dopant cations has proven particularly effective. For example, Ca^{2+}-substituted $LiZr_2(PO_4)_3$, maintaining the rhombohedral NASICON structure, demonstrated a significant improvement in bulk ionic conductivity, reaching up to 1.2×10^{-4} S cm^{-1} at room temperature [29]. Additional studies investigating the effect of composite formation—such as incorporating ZrO_2 or zirconium acetate ($Zr(CH_3COO)_4$)—on the electrical behavior of both pristine $LiZr_2(PO_4)_3$ and Ca-doped analogs (e.g., $Li_{1.4}Ca_{0.2}Zr_{1.8}(PO_4)_3$) revealed that Ca^{2+} incorporation helped stabilize the rhombohedral symmetry without significantly altering the bulk composition of the material. Furthermore, grain boundary conductivity was notably improved, likely due to a reduction in interfacial resistance between crystallites.

Substitution with other dopants such as yttrium has also shown promise. Y^{3+}-doped $LiZr_2(PO_4)_3$ exhibited enhanced structural stability in the rhombohedral phase and achieved a total ionic conductivity of 0.71×10^{-4} S cm^{-1} at 25 °C [30]. These findings reinforce the conclusion that divalent and trivalent cation substitutions, such as Ca^{2+} and Y^{3+}, play an essential role in stabilizing the rhombohedral structure and improving the electrochemical performance at ambient conditions. Comparative analyses further suggest that materials retaining the rhombohedral phase generally exhibit higher conductivities than their counterparts with lower symmetry structures [31].

Beyond structural and conductivity optimization, the interfacial behavior between $LiZr_2(PO_4)_3$ and lithium metal has also been a subject of active investigation. Li and Goodenough [32] explored the interfacial reaction dynamics between Li metal and $LiZr_2(PO_4)_3$ and reported the formation of a stable interphase layer comprising Li_3P and Li_8ZrO_6. This layer was shown to promote wetting at the solid electrolyte–lithium metal interface, a desirable trait for suppressing lithium dendrite formation. A similar interface was observed in Mg-doped compositions such as $Li_{1.2}Mg_{0.1}Zr_{1.9}(PO_4)_3$, where the formation of a Li_3P-rich interphase was also credited with improving interfacial contact and reducing dendritic growth tendencies [33].

Recent computational studies have further deepened the understanding of the electrochemical stability and lithium-ion conduction mechanisms in $LiZr_2(PO_4)_3$ [34]. According to thermodynamic modeling conducted by Li and Goodenough, the material was shown to possess a stable electrochemical window ranging from 2.20 to 4.14 V vs. Li/Li^+, and the lithium insertion potential (or embolism voltage) was found to be thermodynamically favorable. The enhancement in ionic conductivity was attributed to the presence of Frenkel-type defects, which facilitate the mobility of lithium ions through the crystal lattice.

Presently, most studies on $LiZr_2(PO_4)_3$ continue to focus on fine-tuning its crystal structure, optimizing electrical conductivity, and minimizing the interfacial resistance between the solid electrolyte and lithium metal electrodes. In one notable effort, Li and Goodenough's research group developed all-solid-state lithium-ion batteries comprising $LiFePO_4$ cathodes and rhombohedrally structured $LiZr_2(PO_4)_3$ or $Li_{1.2}Mg_{0.1}Zr_{1.9}(PO_4)_3$ electrolytes, demonstrating excellent electrochemical cycling stability and promising applicability in high-performance battery systems [10].

2.2 $LiTi_2(PO_4)_3$

Research into $LiTi_2(PO_4)_3$ as a NASICON-type solid electrolyte began in the 1990s, prompting extensive investigations into its structure and conductivity enhancement. One of the principal strategies for improving ionic conductivity involved partial substitution of Ti^{4+} with trivalent cations (M^{3+}), which

  | DOI: https://doi.org/10.60787/jcas.vol2no1.2| CC BY 4.0

contributed significantly to densification upon sintering and, in turn, enhanced Li^+ transport [35].
Kazakevičius *et al*. (2008) reported the formation of two distinct phases in La-doped $LiTi_2(PO_4)_3$ systems: a NASICON-type structure and $LaPO_4$ as a secondary phase [36]. Their study emphasized that longer sintering times led to reduced porosity, which correlated positively with improved ionic conductivity. Among the substituted variants, Al^{3+}-doped $LiTi_2(PO_4)_3$ has emerged as one of the most extensively studied. Notably, glass-ceramic electrolytes of the form $Li_{1+x}Al_xTi_{2-x}(PO_4)_3$, prepared via melt-quenching, achieved ionic conductivities as high as 1.3×10^{-3} S cm^{-1} at room temperature (RT) [37].
Substituting P^{5+} with elements such as Al^{3+}, Ti^{4+}, and Si^{4+} has also been shown to enhance Li^+ conductivity, potentially reaching values of 10^{-3} S cm^{-1} at RT [38]. However, the stability of these glass-ceramics in aqueous and alkaline environments has proven variable. For example, although stable in $LiNO_3$ and LiCl, the materials degrade under high pH (>10) conditions [39]. Acid treatment (e.g., with acetic or formic acid at 50 °C for 4 months) induced no structural changes detectable via XRD, but did result in a notable reduction in conductivity [40].

Tan *et al*. (2012) successfully fabricated Li–Al–Ti–P–O–N thin films via RF magnetron sputtering, using NASICON-type targets [41]. The highest ionic conductivity, 1.22×10^{-5} S cm^{-1}, was achieved at a coating temperature of 500 °C. Notably, nitrogen incorporation was found to promote cross-linking within the structure, positively impacting ionic conduction. In another study, Peng et al. (2012) used B_2O_3 as a sintering aid to enhance conductivity in $LiTi_2(PO_4)_3$-based materials. The B^{3+} addition increased the lithium content per formula unit and facilitated the formation of dense ceramics [42].
However, concerns remain regarding the reduction of Ti^{4+}, which can lead to undesirable electronic conductivity and compromise the electrochemical stability of the solid electrolyte.

2.3 $LiGe_2(PO_4)_3$-Based NASICON Electrolytes

$LiGe_2(PO_4)_3$ represents another class of NASICON-type solid electrolytes that has attracted considerable attention. Due to the high cost of germanium, research has focused on reducing Ge^{4+} content through partial substitution, particularly using Al^{3+}, leading to the general formula $Li_{1+x}Al_xGe_{2-x}(PO_4)_3$. This aliovalent substitution not only reduced material cost but also substantially increased ionic conductivity—by up to four orders of magnitude—through the generation of additional lithium ions and conduction pathways.
Experimental and computational studies confirmed that increased lithium concentration, enabled by Al^{3+} substitution, was responsible for the conductivity enhancement. However, elevated crystallization temperatures and prolonged crystallization durations were found to negatively affect conductivity by promoting grain growth and reducing grain boundary mobility [43].
Further studies explored the effect of Li_2O excess in $Li_{1+x}Al_xGe_{2-x}(PO_4)_3$ glass-ceramics. The added Li_2O promoted crystallization and served as a nucleation agent, generating a secondary phase that improved interfacial ion transport. A composition such as $Li_{1.5}Al_{0.5}Ge_{1.5}(PO_4)_3$–$0.05Li_2O$ exhibited an overall ionic conductivity of 7.25×10^{-4} S cm^{-1} at RT [44].

Using the hot-pressing technique, a 60 µm thick $Li_{1.5}Al_{0.5}Ge_{1.5}(PO_4)_3$ solid electrolyte was fabricated, achieving 1×10^{-3} S cm^{-1} at 80 °C. This high conductivity value holds promise for lowering internal cell resistance and improving overall battery performance [45]. Recent advancements also include Al and Ti co-substitution in the Ge-based matrix, described by the formula $Li_{1+x+y}Al_x(Ge, Ti)_y(PO_4)_3$. However, the co-existence of Ti and Ge poses risks due to their susceptibility to reduction, which can lead to the formation of conductive interfacial layers and eventual battery failure [46]. In a nutshell, while $Li_{1+x}Al_xGe_{2-x}(PO_4)_3$ shows great promise in terms of ionic conductivity, its practical application is constrained by the high cost of Ge and the instability of Ge^{4+} under reducing conditions. The effectiveness of the electrolyte depends strongly on controlled crystallization parameters and the minimization of reduction-induced degradation.

3.0 THE IMPROVEMENT OF BULK ELECTROLYTES

For NASICON-type solid electrolytes to be viable in practical all-solid-state battery applications, their ionic conductivity at room temperature (RT) must reach at least 10^{-3} S cm^{-1}. Achieving this benchmark requires concerted efforts to enhance bulk and grain boundary conductivity through tailored processing and compositional strategies. To this end, approaches such as optimized mixture methods, advanced sintering technologies, and strategic chemical doping are critical. These methods not only elevate the intrinsic conductivity of the material but also reduce grain boundary resistance, which often poses a significant barrier to efficient ion transport. Moreover, these strategies are essential for overcoming limitations in current synthesis techniques, especially those impeding large-scale production and uniform material performance.

  | DOI: https://doi.org/10.60787/jcas.vol2no1.2|

A notable example of this is the effect of Li_3PO_4 addition on the performance of $Li_{1.3}Al_{0.3}Ti_{1.7}(PO_4)_3$ (LATP) solid electrolytes. The incorporation of Li_3PO_4 in amounts ranging from 0 to 1 wt% has been shown to significantly improve the ionic conductivity of the NASICON-type compound. Specifically, the addition of 1 wt% Li_3PO_4 not only enhances sinterability but also promotes better densification of the electrolyte during processing [47]. This improvement is attributed to a reduction in porosity and more compact grain packing, which collectively minimize interfacial resistance at grain boundaries and facilitate more efficient Li^+ ion migration. The Li_3PO_4 fills voids and reduces pore sizes, thereby enhancing the physical integrity and conductivity of the electrolyte.

Structurally, NASICON-type materials like LATP accommodate Li^+ ions at two crystallographically distinct lattice sites, typically referred to as the M1 cavity and a secondary position known as the M2′ site. Ionic transport involves the migration of Li^+ ions between these sites through narrow bottlenecks formed by the surrounding polyhedral framework [11]. As temperature increases, a greater number of mobile Li^+ ions transition from the M1 to M2′ positions, which facilitates higher conductivity due to increased carrier mobility. For LATP, this thermally activated redistribution leads to a significant enhancement in conductivity, achieving values as high as 6.2×10^{-3} S cm^{-1} at room temperature—well above the threshold needed for practical applications [48, 49].

3.1 Preparation Process

The choice of synthesis and processing routes exerts a profound influence on the ionic conductivity of NASICON-type solid electrolytes. Broadly, two families of methodologies dominate: traditional solid-state reactions [50,51] and a suite of wet-chemical techniques, including sol–gel [52,53], hydrothermal [18,54], co-precipitation [55,56], and Pechini-type sol–gel processes [57,58]. Each approach affords a distinct level of control over phase purity, compositional homogeneity, and particle size, all of which critically determine the electrolyte's microstructure and, ultimately, its conductivity.

Achieving high density and a favorable grain morphology—while minimizing residual porosity—remains a central challenge, particularly for solid-state-derived powders that require prolonged high-temperature sintering [59]. Extended dwell times at elevated temperatures can lead to lithium volatilization and deviation from target stoichiometry, undermining both structural integrity and ion transport. To circumvent these limitations, advanced consolidation techniques such as spark plasma sintering (SPS) have been adopted, enabling rapid densification at lower thermal budgets and yielding NASICON electrolytes with markedly enhanced performance [9,60–62].

For practical all-solid-state lithium-ion battery applications, a room-temperature ionic conductivity exceeding 10^{-3} S cm^{-1} is often cited as the benchmark. However, conventional solid-state reaction routes typically deliver conductivities on the order of 10^{-4} S cm^{-1}. Figure 3.1 presents a comparative flowchart of the solid-state and wet-chemical synthesis pathways for NASICON-type solid electrolytes, highlighting their respective process steps and critical parameters.

  DOI: https://doi.org/10.60787/jcas.vol2no1.2|

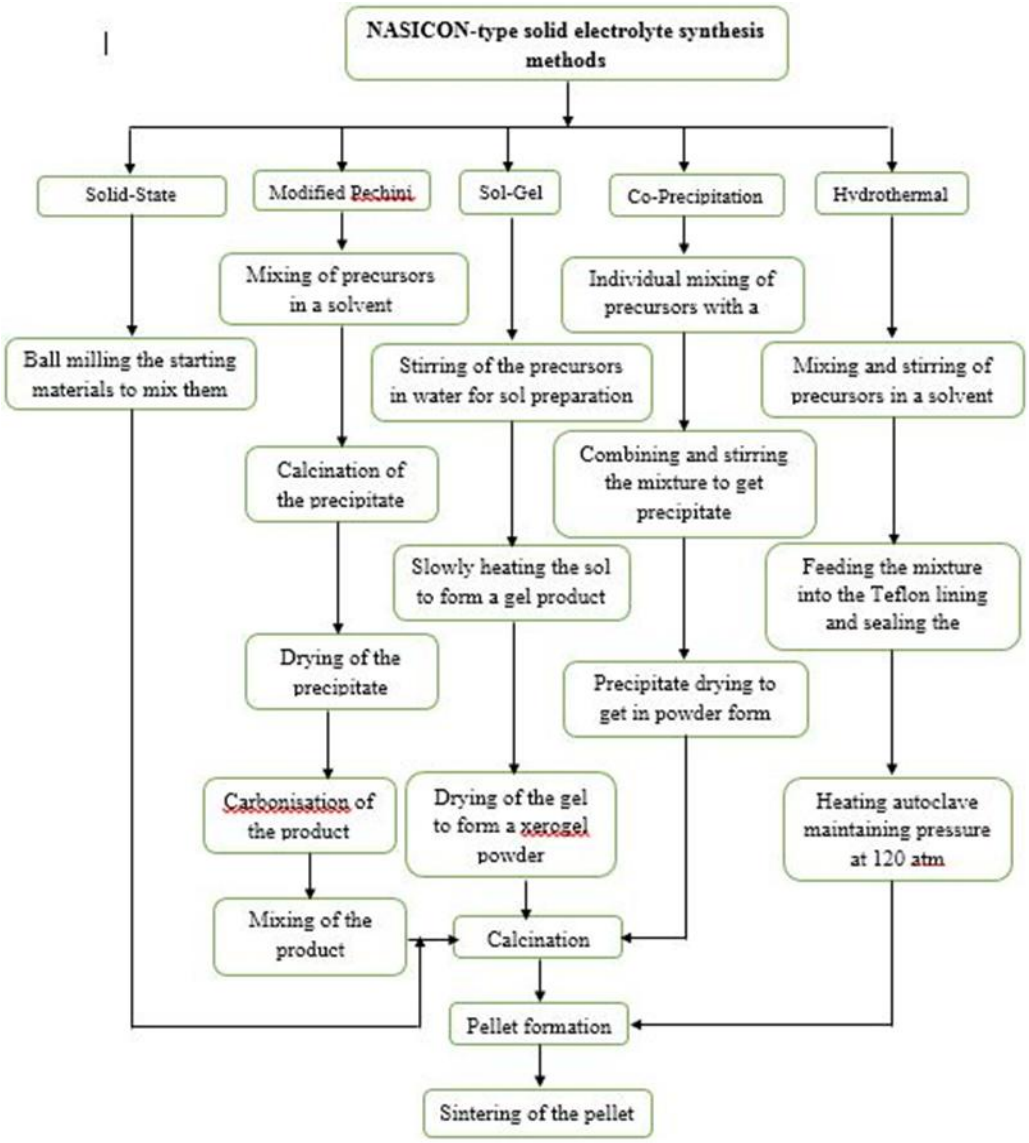

Figure 3.1: Flowchart of the solid-state reaction and wet-chemical methods of synthesizing NASICON-type solid electrolytes.

  DOI: https://doi.org/10.60787/jcas.vol2no1.2|

The key findings regarding lithium-containing NASICONs synthesized using this approach are outlined in Table 3.1.

Table 3.1: Ionic conductivities of NASICON-type solid electrolyte produced by solid-state reaction method.

Chemical Composition	Ionic Conductivity (S cm^{-1})	References
$Li_2Ge_2(PO_4)_3$	7.2 x 10^{-7} (900 ^{0}C)	Feng *et al*., 2009 [63]
$Li_{1.5}Al_{0.5}Ge_{1.5}(PO_4)_3$	2.4 x 10^{-4} (900 – 1000 ^{0}C)	Aono *et al*., 1992 [64]
$Li_{1.5}Al_{0.5}Ge_{1.5}(PO_4)_3$	7. 0 x 10^{-5} (850 ^{0}C)	Liu *et al*., 2018 [65]
$Li_{1.5}Cr_{0.5}Ge_{1.5}(PO_4)_3$	1.3 x 10^{-4} (900 – 1000 ^{0}C)	Aono *et al*., 1992 [64]
$Li_2CrHf(PO_4)_3$	4.2 x 10^{-8} (1100 – 1200 ^{0}C)	Sugantha &Varadaraju, 1997 [66]
$Li_2InHf(PO_4)_3$	2.7 x 10^{-8} (1100 – 1200 ^{0}C)	Sugantha & Varadaraju, 1997 [66]
$Li_2CrZr(PO_4)_3$	5.9 x 10^{-7} (1100 – 1200 ^{0}C)	Sugantha & Varadaraju, 1997 [66]
$Li_2FeZr(PO_4)_3$	1.4 x 10^{-7} (1100 – 1200 ^{0}C)	Sugantha & Varadaraju, 1997 [66]
$Li_2InZr(PO_4)_3$	8.2 x 10^{-8} (1100 – 1200 ^{0}C)	Sugantha & Varadaraju, 1997 [66]
$LiTi_2(PO_4)_3$	7.20 x 10^{-5} (1050 ^{0}C)	Venkateswara *et al.* 2015 [67]
$Li_{1.4}Ti_{1.9}(PO_4)_3$	2.65 x 10^{-6} (800 ^{0}C)	Kahlaoui *et al*., 2020 [68]
$Li_{1.3}Al_{0.3}Ti_{1.7}(PO_4)_3$	3.15 x 10^{-4} (890 ^{o}C)	Hallopeau *et al.,* 2018 [61]
$Li_{1.3}Al_{0.3}Ti_{1.7}(PO_4)_3$	1.34 x 10^{-6} (1200 ^{0}C)	Belous *et al*., 2018 [69]
$Li_{1.2}Al_{1.1}Ta_{0.9}(PO_4)_3$	9.854 x 10^{-6} (800 ^{0}C)	Mohammed *et al*., 2018 [50]
$Li_{0.9}V_{0.1}Ti_{1.9}(PO_4)_3$	4.26 x 10^{-4} (1050 ^{0}C)	Venkateswara *et al.,* 2014 [70]
$Li_{1.3}Al_{0.3}Ti_{1.7}(PO_4)_3 + LiTiPO_5$	2.9 x 10^{-4} (800 ^{0}C)	Li & Zhao, 2019 [71]
$Li_{0.5}Nb_{0.5}Ti_{1.5}(PO_4)_3$	6.02 x 10^{-9} (850 ^{0}C)	Kahlaoui *et al*., 2018 [72]
$Li_2CrTi(PO_4)_3$	4.4 x 10^{-7} (1100 – 1200 ^{0}C)	Sugantha & Varadaraju, 1997 [66]
$Li_2FeTi(PO_4)_3$	3.34 x 10^{-7} (1100 – 1200 ^{0}C)	Sugantha & Varadaraju, 1997 [66]
$Li_2InTi(PO_4)_3$	8.30 x 10^{-6} (1100 – 1200 ^{0}C)	Sugantha & Varadaraju, 1997 [66]
$Li_2Zr_{0.1}Ti_{1.9}(PO_4)_3$	4.68 x 10^{-5} (1050 ^{0}C)	Venkateswara *et al.,* 2014 [70]
$Li_{1.15}Ti_{1.85}Fe_{0.15}(PO_4)_3$	5.22 x 10^{-4} (1050 ^{0}C)	Venkateswara *et al.,* 2015 [67]
$Li_{1.2}Fe_{0.3}Hf_{1.7}(PO_4)_3$	5.6 x 10^{-5} (1020 ^{0}C)	Aono *et al*., 1993 [73]
$Li_{1.3}Sc_{0.3}Hf_{1.7}(PO_4)_3$	9.1 x 10^{-5} (1020 ^{0}C)	Aono *et al*., 1993 [73]
$Li_{1.3}In_{0.3}Hf_{1.7}(PO_4)_3$	1.3 x 10^{-4} (1020 ^{0}C)	Aono *et al*., 1993 [73]
$Li_{1.8}Sc_{0.8}Ti_{1.2}(PO_4)_3$	9.98 x 10^{-5} (850 ^{0}C)	Kahlaoui *et al*., 2017 [74]
$Li_{1.2}Ca_{0.1}Zr_{1.9}(PO_4)_3$	1.2 x 10^{-7} (700 ^{0}C)	Cassel *et al*., 2017 [75]
$Li_{1.275}Al_{0.275}Zr_{1.725}(PO_4)_3$	3.06 x 10^{-6} (1200 ^{0}C)	Zhang *et al*., 2017 [76]
$Li_{1.4}Ca_{0.2}Zr_{1.8}(PO_4)_3$	4.2 x 10^{-5} (1150 ^{0}C)	Hanghofer *et al*., 2019 [30]

Notably, powders produced through solid-state synthesis tend to be coarse, lack chemical uniformity, and can pose challenges during sintering, often resulting in the presence of significant secondary phases. Therefore, employing wet-chemical techniques for powder synthesis is crucial for enhancing lithium-ion conductivity. A concise overview of wet-chemical methods is provided in Table 3.2.

 DOI: https://doi.org/10.60787/jcas.vol2no1.2|

Table 3.2: Ionic conductivities of NASICON-type solid electrolyte synthesized by wet-chemical methods.

Chemical Composition	Preparation Techniques	Ionic Conductivity (S cm^{-1})	References
$Li_2Ge_2Sn(PO_4)_3$	modified pechini method	9.4 x 10^{-9} (900 ^{0}C)	Francisco *et al*., 2014 [77]
$Li_{1.5}Al_{0.5}Ge_{0.75}Sn_{0.75}(PO_4)_3$	modified pechini method	1.3 x 10^{-4} (900 ^{0}C)	Francisco *et al*., 2014 [77]
$Li_{1.3}Al_{0.3}Ti_{1.7}(PO_4)_3$	modified pechini method	6.0 x 10^{-4} (900 ^{0}C)	Zhao *et al.,* 2016 [25]
$Li_{1.3}Al_{0.3}Ti_{1.7}(PO_4)_3$	sol-gel	4.2 x 10^{-4} (1000 ^{0}C)	Yi *et al*., 2019 [78]
$Li_{1.4}Al_{0.4}Ti_{1.6}(PO_4)_3$	modified pechini method	3.6 x 10^{-4} (850 ^{0}C)	Xu *et al*., 2008 [79]
$Li_{1.4}Al_{0.4}Ti_{1.6}(PO_4)_3$	modified pechini method	1.12 x 10^{-3} (650 ^{0}C)	Xu *et al*., 2008 [79]
$Li_{1.5}Al_{0.5}Ti_{1.5}(PO_4)_3$	sol-gel	3.4 x 10^{-3} (850 – 950 ^{0}C)	Breuer *et al*., 2015 [80]
$Li_{1.4}Al_{0.4}Ti_{1.6}(PO_4)_3$	sol-gel	1.77 x 10^{-4} (880 – 950 ^{0}C)	Zhang *et al.*, 2013 [81]
$Li_{1.5}Al_{0.5}Ge_{1.5}(PO_4)_3$	sol-gel	3.1 x 10^{-4} (850 ^{0}C)	Liu *et al*., 2018 [65]
$Li_{1.5}Al_{0.5}Ge_{1.5}(PO_4)_3$	enhanced pechini method	1.67 x 10^{-4} (800 ^{0}C)	Zhu *et al*., 2020 [57]
$Li_{1.5}Al_{0.5}Ge_{1.5}(PO_4)_3$	modified pechini method	9.56 x 10^{-5} (600 ^{0}C)	Zhu *et al*., 2020 [57]
$Li_{1.4}Al_{0.4}Ti_{1.4}Ge_{0.2}(PO_4)_3$	sol-gel	1.3 x 10^{-3} (880 – 950 ^{0}C)	Zhang *et al.*, 2013 [81]
$Li_{1.3}Al_{0.3}Ti_{1.7}(PO_4)_3$	Hydrothermal	4.8 x 10^{-4} (900 ^{0}C)	He *et al*., 2018 [18]
$Li_{1.4}Al_{0.4}Ti_{1.6}(PO_4)_3$	Coprecipitation	1.83 x 10^{-4} (900 ^{0}C)	Huang *et al*., 2011 [56]
$Li_{1.3}Al_{0.3}Ti_{1.7}(PO_4)_3$	Coprecipitation	1.6 x 10^{-4} (850 ^{0}C)	Duluard *et al*., 2013 [55]
$Li_{1.05}Y_{0.05}Ti_{1.95}(PO_4)_3$	enhanced pechini method	2.87 x 10^{-7} (1200 ^{0}C)	Mariappan *et al*., 2018 [58]
$Li_{1.2}Y_{0.2}Ti_{1.8}(PO_4)_3$	enhanced pechini method	6.5 x 10^{-6} (1200 ^{0}C)	Mariappan *et al*., 2018 [58]
$Li_{1.4}Zr_2(PO_4)_3$	sol-gel	2.7 x 10^{-9} (1200 ^{0}C)	Cassel *et al.,* 2017 [75]
$Li_{1.2}Ca_{0.1}Zr_{1.9}(PO_4)_3$	sol-gel	7.17 x 10^{-7} (1200 ^{0}C)	Cassel *et al.,* 2017 [75]
$Li_{1.1}La_{0.2}Zr_{1.9}(PO_4)_3$	enhanced pechini method	7.23 x 10^{-5} (1400 ^{0}C)	Ramar *et al*., 2018 [82]
$Li_{1+x}Al_xTi_{2-x}(PO_4)_3$	sol-gel	7.936 x 10^{-4} (950 ^{0}C)	Mohammed *et al*., 2017 [83]

The occurrence of a liquid phase improves the chemical uniformity of precursors, while lower synthesis temperatures prevent particle growth [59]. The conductivities observed are consistent with those achieved through solid-state reactions. However, certain experiments have shown conductivity levels as low as 10^{-3} S cm^{-1} by integrating wet-chemical methods with spark plasma sintering (SPS) [79] or utilizing CS [81]. In contrast, the focus has shifted towards spark plasma sintering (SPS) for the preparation of NASICON samples [62, 84, 85]. An exceptionally efficient approach for densifying lithium-ion NASICON involves pressing and sintering techniques, including Pulsed Electric Current Sintering, which employs electric current pulses and uniaxial pressure during sintering. This technique enables rapid densification at lower temperatures and shorter durations compared to traditional sintering methods [9]. A relative density exceeding 95% has been achieved for the $Li_{1.3}Fe_{0.3}Ti_{1.7}(PO_4)_3$ material at temperatures as low as 600 °C using this method [84]. Additionally, the $Li_{1.4}Al_{0.1}Ti_{1.6}(PO_4)_3$ material with a conductivity of up to 1.12 × 10^{-3} S cm^{-1} at room temperature has been successfully developed, meeting the minimum requirement for battery applications (10^{-3} S cm^{-1}). This outcome represents a dense integration of nanotechnology in powder processing combined with SPS, achieving 100% theoretical density [79].

3.2 Chemical Doping

Substitution strategies in NASICON-type lithium conductors have played a pivotal role in enhancing their ionic conductivity and electrochemical stability. One such approach involves replacing a tetravalent cation such as Ge^{4+} with a trivalent cation like Al^{3+} in the crystal lattice. This aliovalent substitution necessitates the incorporation of additional Li^+ ions into the structure to maintain charge neutrality. These excess lithium ions are believed to occupy the M2 interstitial sites, which are accessible within the NASICON framework due to its open three-dimensional network [55]. Consequently, the stoichiometry of these materials is often represented as $Li_{1+x}M_x^{III}M_{2-x}^{IV}(PO_4)_3$, where the value of x corresponds to the amount of trivalent substitution and

  | DOI: https://doi.org/10.60787/jcas.vol2no1.2|

the number of compensating lithium ions. This systematic increase in lithium concentration contributes significantly to improved ionic conductivity, as Li^+ ions migrate between occupied and unoccupied interstitial sites more efficiently [77, 86].

The ionic conductivity (σ) of such materials is quantitatively described by the relation σ = cμq, where *c* is the concentration of mobile charge carriers, *μ* is their mobility, and *q* is the charge on the ion [87]. Therefore, enhancing *c* through compositional tuning directly translates to higher conductivity. However, the permissible extent of trivalent cation incorporation (x) without inducing adverse structural distortions or the formation of secondary phases is highly dependent on the chemical nature of the dopant and the structural compatibility with the host matrix [12]. The effectiveness of Al^{3+} in particular has been attributed not only to its charge contribution but also to its ionic radius (0.53 nm), which is close to that of Ti^{4+} (0.605 nm). This similarity facilitates its incorporation without significantly distorting the crystal lattice, thus preserving mechanical stability and conductive pathways.

In contrast, while Ti^{4+} is a common host cation in NASICON-type structures such as $LiTi_2(PO_4)_3$, it is prone to reduction by metallic lithium, which can lead to the undesirable formation of electronically conductive phases and jeopardize the long-term stability of solid-state batteries. To address this issue, alternative high-valence dopants like tantalum (Ta^{5+}) have been explored. Ta^{5+}, with an ionic radius of 0.64 nm, falls within the acceptable tolerance for substitution and exhibits superior chemical and electrochemical stability when in contact with lithium. It also maintains structural compatibility with other framework cations such as Al^{3+} and Ti^{4+}, enabling the development of doped NASICON compositions that retain high ionic conductivities without sacrificing stability [50]. The judicious selection and substitution of dopants thus provide a strategic avenue for optimizing the performance of NASICON-type solid electrolytes for next-generation lithium-ion and lithium-metal battery systems.

4.0 CONCLUSION

The resulting battery with optimized capacity and safety could be an all-solid-state battery. Due to their excellent ionic conductivity and stability, solid electrolytes of the NASICONs-type have attracted a lot of scientific attention. The primary advancements addressed in this review can be encapsulated in the following key elements:

(1) Experimental research in the field has revealed the best-conducting properties for $LiTi_2(PO_4)_3$ and $LiGe_2(PO_4)_3$-based systems.
(2) Electrolytes synthesized through solid-state reactions often face difficulties in achieving high densities.
(3) Nonconventional techniques were utilized to develop densification, with SPS (Spark Plasma Sintering) yielding the most promising results.
(4) Wet-chemical methods have been instrumental in producing NASICON (Sodium Superionic Conductor) with complex compositions, smaller particle sizes, and improved chemical homogeneity.
(5) Electrolytes synthesized through wet-chemical methods achieve greater conductivity than those produce by standard solid-state synthesis.
(6) This review outlines the transition from flammable liquid electrolytes to solid ceramic materials in lithium-ion batteries (LIBs). The advancement of LIBs for electronics and electric vehicle (EV) applications hinges on enhancing both electrode materials and electrolytes to enhance specific energies.

Authors' Declaration

The authors certify that this research is original, has not been published previously, and is not under consideration by any other journal. We assume full responsibility for the integrity of the data and the accuracy of the reported findings and will accept all liability for any claims about the content

Conflict of Interest

The authors declare that they have no conflict of interest.

Data Availability Statement

All data supporting this study are available upon request from the corresponding author.

Authors' Contribution

Mohammed Isah Kimpa: original draft writing and funding acquisition. Abubakar Sadiq Sanda & Abubakar Sadiq Yusuf: writing review and editing. Akoba Rashidah, Jibrin Alhaji Yabagi, Muhammad Bello Ladan & Abubakar Shehu Kollere: conceptualization and methodology. Haruna Isah: Validation and analysis. Muhammad Muhammad Ndamitso & Kasim Uthman Isah: review, editing and Supervision.

Ethical Declarations Human/Animal Studies

The authors declare that no human/animal was used for the studies

 DOI: https://doi.org/10.60787/jcas.vol2no1.2|

Acknowledgments
The authors gratefully acknowledge the Department of Chemical Engineering, Federal University of Petroleum Resources, Effurun (FUPRE), for providing the research facilities and enabling environment that supported this work. Special appreciation goes to the dedicated laboratory staff for their technical assistance and valuable contributions during experimental procedures. We also extend our sincere gratitude to the Mechanical Engineering Department's workshop team for their expertise in sample preparation and equipment maintenance. Their collective support was instrumental to the success of this study. Finally, we thank all colleagues and researchers whose insightful discussions helped refine this work**.** The authors acknowledge the use of DeepSeek Chat (DeepSeek, 2025) for language refinement and Canva for graphic design assistance. These tools were used solely to enhance manuscript clarity, readability, and visual presentation. The use of these methods did not impact the scientific integrity, data analysis, or conclusions of this study.

REFERENCES

[1] Z. Zhang, X. Wang, X. Li, J. Zhao, G. Liu, W. Yu, *et al.*, "Review on composite solid electrolytes for solid-state lithium-ion batteries," *Mater. Today Sustain.*, vol. 21, p. 100316, Mar. 2023, doi: 10.1016/j.mtsust.2023.100316.

[2] M. Ma, M. Zhang, B. Jiang, Y. Du, B. Hu, and C. Sun, "A review of all-solid-state electrolytes for lithium batteries: high-voltage cathode materials, solid-state electrolytes and electrode-electrolyte interfaces," *Mater. Chem. Front.*, vol. 7, no. 7, pp. 1268–1297, 2023, doi: 10.1039/D2QM01071B.

[3] C. Li, R. Li, K. Liu, R. Si, Z. Zhang, and Y. Hu, "NaSICON: A promising solid electrolyte for solid-state sodium batteries," *Interdiscip. Mater.*, vol. 1, no. 3, pp. 396–416, 2022, doi: 10.1002/idm2.12044.

[4] J. Jiang and J. Liu, "Iron anode-based aqueous electrochemical energy storage devices: recent advances and future perspectives," *Interdiscip. Mater.*, vol. 1, no. 1, pp. 116–139, 2022, doi: 10.1002/idm2.12007.

[5] N. Boaretto, I. Garbayo, S. Valiyaveettil-SobhanRaj, A. Quintela, C. Li, M. Casas-Cabanas *et al.*, "Lithium solid-state batteries: State-of-the-art and challenges for materials, interfaces and processing," *J. Power Sources*, vol. 502, p. 229919, 2021, doi: 10.1016/j.jpowsour.2021.229919.

[6] C. Li, Z. Wang, Z. He, Y. Li, J. Mao, K. Dai, *et al.*, "An advance review of solid-state battery: Challenges, progress and prospects," *Sustain. Mater. Technol.*, vol. 29, p. e00297, 2021, doi: 10.1016/j.susmat.2021.e00297.

[7] L. Wang, J. Li, G. Lu, W. Li, Q. Tao, C. Shi *et al.*, "Fundamentals of electrolytes for solid-state batteries: challenges and perspectives," *Front. Mater.*, vol. 7, p. 111, 2020, doi: 10.3389/fmats.2020.00111.

[8] G. Yang, C. Abraham, Y. Ma, M. Lee, E. Helfrick, D. Oh, *et al.*, "Advances in materials design for all-solid-state batteries: from bulk to thin films," *Appl. Sci.*, vol. 10, no. 14, p. 4727, 2020, doi: 10.3390/app10144727.

[9] H. Zhu, A. Prasad, S. Doja, L. Bichler, and J. Liu, "Spark plasma sintering of lithium aluminum germanium phosphate solid electrolyte and its electrochemical properties," *Nanomaterials*, vol. 9, no. 8, p. 1086, 2019, doi: 10.3390/nano9081086.

[10] L. Zhang, Y. Liu, Y. You, A. Vinu, and L. Mai, "NASICONs-type solid-state electrolytes: The history, physicochemical properties, and challenges," *Interdiscip. Mater.*, vol. 2, no. 1, pp. 91–110, 2023, doi: 10.1002/idm2.12046.

[11] A. Jonderian and E. McCalla, "The role of metal substitutions in the development of Li batteries, part II: solid electrolytes," *Mater. Adv.*, vol. 2, no. 9, pp. 2846–2875, 2021, doi: 10.1039/D1MA00082A.

[12] J. A. Dias, S. H. Santagneli, and Y. Messaddeq, "Methods for lithium ion NASICON preparation: from solid-state synthesis to highly conductive glass-ceramics," *J. Phys. Chem. C*, vol. 124, no. 49, pp. 26518–26539, 2020, doi: 10.1021/acs.jpcc.0c07385.

[13] A. Banik, T. Famprikis, M. Ghidiu, S. Ohno, M. A. Kraft, and W. G. Zeier, "On the underestimated influence of synthetic conditions in solid ionic conductors," *Chem. Sci.*, vol. 12, no. 18, pp. 6238–6263, 2021, doi: 10.1039/D0SC06553F.

[14] D. C. Gunduz, R. Schierholz, S. Yu, H. Tempel, H. Kungl, and R.-A. Eichel, "Combined quantitative microscopy on the microstructure and phase evolution in $Li_{1.3}Al_{0.3}Ti_{1.7}(PO_4)_3$ ceramics," *J. Adv. Ceram.*, vol. 9, pp. 149–161, 2020, doi: 10.1007/s40145-019-0354-0.

[15] A. Rossbach, F. Tietz, and S. Grieshammer, "Structural and transport properties of lithium-conducting NASICON materials," *J. Power Sources*, vol. 391, pp. 1–9, 2018, doi: 10.1016/j.jpowsour.2018.04.059.

[16] F. Zheng, M. Kotobuki, S. Song, M. O. Lai, and L. Lu, "Review on solid electrolytes for all-solid-state lithium-ion batteries," *J. Power Sources*, vol. 389, pp. 198–213, 2018, doi: 10.1016/j.jpowsour.2018.04.022.

[17] D. H. S. Tan, A. Banerjee, Z. Chen, and Y. S. Meng, "From nanoscale interface characterization to sustainable energy storage using all-solid-state batteries," *Nat. Nanotechnol.*, vol. 15, no. 3, pp. 170–180, 2020, doi: 10.1038/s41565-020-0657-x.

  DOI: https://doi.org/10.60787/jcas.vol2no1.2|

[18] S. He, Y. Xu, B. Zhang, X. Sun, Y. Chen, and Y. Jin, "Unique rhombus-like precursor for synthesis of $Li_{1.3}Al_{0.3}Ti_{1.7}(PO_4)_3$ solid electrolyte with high ionic conductivity," *Chem. Eng. J.*, vol. 345, pp. 483–491, 2018, doi: 10.1016/j.cej.2018.03.151.
[19] Y. Arinicheva, M. Wolff, S. Lobe, C. Dellen, D. Fattakhova-Rohlfing, O. Guillon *et al.*, "Ceramics for electrochemical storage," in *Advanced ceramics for energy conversion and storage*, Elsevier, 2020, pp. 549–709, doi: 10.1016/B978-0-08-102726-4.00010-7.
[20] L. Liu, D. Zhang, X. Xu, Z. Liu, and J. Liu, "Challenges and development of composite solid electrolytes for all-solid-state lithium batteries," *Chem. Res. Chinese Univ.*, vol. 37, pp. 210–231, 2021, doi: 10.1007/s40242-021-0007-z.
[21] M. Hou, F. Liang, K. Chen, Y. Dai, and D. Xue, "Challenges and perspectives of NASICON-type solid electrolytes for all-solid-state lithium batteries," *Nanotechnology*, vol. 31, no. 13, p. 132003, 2020, doi: 10.1088/1361-6528/ab5be7.
[22] S. Sharma, V. Singh, R. K. Kotnala, and R. K. Dwivedi, "Comparative studies of pure BiFeO 3 prepared by sol–gel versus conventional solid-state-reaction method," *J. Mater. Sci. Mater. Electron.*, vol. 25, pp. 1915–1921, 2014, doi: 10.1007/s10854-014-1820-7.
[23] Y. B. Rao, K. K. Bharathi, and L. N. Patro, "Review on the synthesis and doping strategies in enhancing the Na ion conductivity of $Na_3Zr_2Si_2PO_{12}$ (NASICON) based solid electrolytes," *Solid State Ionics*, vol. 366, p. 115671, 2021, doi: 10.1016/j.ssi.2021.115671.
[24] C. R. Mariappan, C. Galven, M.-P. Crosnier-Lopez, F. Le Berre, and O. Bohnke, "Synthesis of nanostructured $LiTi_2(PO_4)_3$ powder by a Pechini-type polymerizable complex method," *J. Solid State Chem.*, vol. 179, no. 2, pp. 450–456, 2006, doi: 10.1016/j.jssc.2005.11.005.
[25] E. Zhao, F. Ma, Y. Jin, and K. Kanamura, "Pechini synthesis of high ionic conductivity $Li_{1.3}Al_{0.3}Ti_{1.7}(PO_4)_3$ solid electrolytes: The effect of dispersant," *J. Alloys Compd.*, vol. 680, pp. 646–653, 2016, doi: 10.1016/j.jallcom.2016.04.173.
[26] J. B. Goodenough, H.-P. Hong, and J. A. Kafalas, "Fast Na^+-ion transport in skeleton structures," *Mater. Res. Bull.*, vol. 11, no. 2, pp. 203–220, 1976, doi: 10.1016/0025-5408(76)90077-5.
[27] N. a Anantharamulu, K. Koteswara Rao, G. Rambabu, B. Vijaya Kumar, V. Radha, and M. Vithal, "A wide-ranging review on Nasicon type materials," *J. Mater. Sci.*, vol. 46, pp. 2821–2837, 2011, doi: 10.1007/s10853-011-5302-5.
[28] M. I. Kimpa, M. Z. H. Mayzan, J. A. Yabagi, M. M. Nmaya, K. U. Isah, and M. A. Agam, "Review on material synthesis and characterization of sodium (Na) super-ionic conductor (NASICON)," in *IOP Conference Series: Earth and Environmental Science*, 2018, vol. 140, no. 1, p. 12156, doi: 10.1088/1755-1315/140/1/012156.
[29] H. Xie, J. B. Goodenough, and Y. Li, "$Li_{1.2}Zr_{1.9}Ca_{0.1}(PO_4)_3$, a room-temperature Li-ion solid electrolyte," *J. Power Sources*, vol. 196, no. 18, pp. 7760–7762, 2011, doi: 10.1016/j.jpowsour.2011.05.002.
[30] I. Hanghofer, B. Gadermaier, A. Wilkening, D. Rettenwander, and H. M. R. Wilkening, "Lithium ion dynamics in $LiZr_2(PO_4)_3$ and $Li_{1.4}Ca_{0.2}Zr_{1.8}(PO_4)_3$," *Dalt. Trans.*, vol. 48, no. 25, pp. 9376–9387, 2019, doi: 10.1039/C9DT01786K.
[31] Y. Li, M. Liu, K. Liu, and C. A. Wang, "High Li^+ conduction in NASICON-type $Li_{1+x}Y_xZr_{2-x}(PO_4)_3$ at room temperature," *J. Power Sources*, vol. 240, pp. 50–53, 2013, doi: 10.1016/j.jpowsour.2013.03.175.
[32] Y. Li, W. Zhou, X. Chen, X. Lü, Z. Cui, S. Xin, *et al.*, "Mastering the interface for advanced all-solid-state lithium rechargeable batteries," *Proc. Natl. Acad. Sci.*, vol. 113, no. 47, pp. 13313–13317, 2016, doi: 10.1073/pnas.161591211.
[33] Q. Zhou, B. Xu, P. H. Chien, Y. Li, B. Huang, N. Wu, *et al.*, "NASICON $Li_{1.2}Mg_{0.1}Zr_{1.9}(PO_4)_3$ solid electrolyte for an all-solid-state Li-metal battery," *Small Methods*, vol. 4, no. 12, p. 2000764, 2020, doi: 10.1002/smtd.202000764.
[34] Y. Noda, K. Nakano, H. Takeda, M. Kotobuki, L. Lu, and M. Nakayama, "Computational and experimental investigation of the electrochemical stability and Li-ion conduction mechanism of $LiZr_2(PO_4)_3$," *Chem. Mater.*, vol. 29, no. 21, pp. 8983–8991, 2017, doi: 10.1021/acs.chemmater.7b01703.
[35] H. AONO, "Ionic conductivity and sinterability of lithium titanium phosphate system," *Solid State Ionics*, vol. 40–41, pp. 38–42, Aug. 1990, doi: 10.1016/0167-2738(90)90282-V.
[36] E. Kazakevicius, T. Šalkus, A. Dindune, Z. Kanepe, J. Ronis, A. Kežionis, *et al.*, "La-doped $LiTi_2(PO_4)_3$ ceramics," *Solid State Ionics*, Feb. 2008, doi: 10.1016/j.ssi.2007.12.025.
[37] J. Fu, "Superionic conductivity of glass-ceramics in the system Li_2O-Al_2O_3-TiO_2-P_2O_5," *Solid State Ionics*, vol. 96, no. 3–4, pp. 195–200, Apr. 1997, doi: 10.1016/S0167-2738(97)00018-0.
[38] J. Fu, "Fast Li^+ Ion Conduction in Li_2O-Al_2O_3-TiO_2-SiO_2-P_2O_2 Glass-Ceramics," *J. Am. Ceram. Soc.*, vol. 80, no. 7, pp. 1901–1903, Jul. 1997, doi: 10.1111/j.1151-2916.1997.tb03070.x.
[39] Y. Shimonishi, T. Zhang, N. Imanishi, D. Im, D. J. Lee, A. Hirano, *et al.*, "A study on lithium/air secondary batteries—Stability of the NASICON-type lithium ion conducting solid electrolyte in alkaline aqueous solutions," *J. Power Sources*, vol. 196, no. 11, pp. 5128–5132, Jun. 2011, doi: 10.1016/j.jpowsour.2011.02.023.

  DOI: https://doi.org/10.60787/jcas.vol2no1.2|

[40] Y. Shimonishi, T. Zhang, P. Johnson, N. Imanishi, A. Hirano, Y. Takeda, *et al.*, "A study on lithium/air secondary batteries—Stability of NASICON-type glass ceramics in acid solutions," *J. Power Sources*, vol. 195, no. 18, pp. 6187–6191, Sep. 2010, doi: 10.1016/j.jpowsour.2009.11.023.

[41] G. Tan, F. Wu, L. Li, Y. Liu, and R. Chen, "Magnetron Sputtering Preparation of Nitrogen-Incorporated Lithium–Aluminum–Titanium Phosphate Based Thin Film Electrolytes for All-Solid-State Lithium Ion Batteries," *J. Phys. Chem. C*, vol. 116, no. 5, pp. 3817–3826, Feb. 2012, doi: 10.1021/jp207120s.

[42] H. Peng, H. Xie, and J. B. Goodenough, "Use of B_2O_3 to improve Li^+-ion transport in $LiTi_2(PO_4)_3$-based ceramics," *J. Power Sources*, vol. 197, pp. 310–313, Jan. 2012, doi: 10.1016/j.jpowsour.2011.09.046.

[43] J. S. Thokchom and B. Kumar, "The effects of crystallization parameters on the ionic conductivity of a lithium aluminum germanium phosphate glass–ceramic," *J. Power Sources*, vol. 195, no. 9, pp. 2870–2876, May 2010, doi: 10.1016/j.jpowsour.2009.11.037.

[44] X. Xu, Z. Wen, X. Wu, X. Yang, and Z. Gu, "Lithium Ion-Conducting Glass–Ceramics of $Li_{1.5}Al_{0.5}Ge_{1.5}(PO_4)_3$–x Li_2O (x =0.0–0.20) with Good Electrical and Electrochemical Properties," *J. Am. Ceram. Soc.*, vol. 90, no. 9, pp. 2802–2806, Sep. 2007, doi: 10.1111/j.1551-2916.2007.01827.x.

[45] A. Paolella, W. Zhu, G. Bertoni, A. Perea, H. Demers, S. Savoie, *et al.*, "Toward an All-Ceramic Cathode–Electrolyte Interface with Low-Temperature Pressed NASICON $Li_{1.5}Al_{0.5}Ge_{1.5}(PO_4)_3$ Electrolyte," *Adv. Mater. Interfaces*, vol. 7, no. 12, Jun. 2020, doi: 10.1002/admi.202000164.

[46] P. Hartmann, T. Leichtweiss, M. R. Busche, M. Schneider, M. Reich, J. Sann, *et al.*, "Degradation of NASICON-Type Materials in Contact with Lithium Metal: Formation of Mixed Conducting Interphases (MCI) on Solid Electrolytes," *J. Phys. Chem. C*, vol. 117, no. 41, pp. 21064–21074, Oct. 2013, doi: 10.1021/jp4051275.

[47] Y.-Y. Sun, Q. Zhang, L. Yan, T.-B. Wang, and P.-Y. Hou, "A review of interfaces within solid-state electrolytes: fundamentals, issues and advancements," *Chem. Eng. J.*, vol. 437, p. 135179, Jun. 2022, doi: 10.1016/j.cej.2022.135179.

[48] L. Xu, J. Li, W. Deng, H. Shuai, S. Li, Z. Xu, *et al.*, "Garnet Solid Electrolyte for Advanced All-Solid-State Li Batteries," *Adv. Energy Mater.*, vol. 11, no. 2, Jan. 2021, doi: 10.1002/aenm.202000648.

[49] K. Subramanian, G. V. Alexander, K. Karthik, S. Patra, M. S. Indu, O. V. Sreejith, *et al.*, "A brief review of recent advances in garnet structured solid electrolyte based lithium metal batteries," *J. Energy Storage*, vol. 33, p. 102157, Jan. 2021, doi: 10.1016/j.est.2020.102157.

[50] M. I. Kimpa, M. Z. H. Bin Mayzan, F. Esa, J. A. Yabagi, M. M. Nmaya, and M. A. Bin Agam, "Physical characterization and electrical conductivity of $Li_{1.2}Ti_{1.8}Al_{0.2}(PO_4)_3$ and $Li_{1.2}Ta_{0.9}Al_{1.1}(PO_4)_3$ NASICON material," *Int. J. Integr. Eng.*, vol. 10, no. 9, Dec. 2018, doi: 10.30880/ijie.2018.10.09.020.

[51] T. Zangina, J. Hassan, K. A. Matori, R. S. Azis, C. E. Ndikilar, and F. H. Naning, "Dielectric Relaxation Analysis of Chemical Solid Electrolyte Lithium Aluminum Titanium Phosphate," *Asian J. Appl. Sci.*, vol. 11, no. 1, pp. 46–55, Dec. 2017, doi: 10.3923/ajaps.2018.46.55.

[52] M. Niazmand, Z. Khakpour, and A. Mortazavi, "Electrochemical properties of nanostructure NASICON synthesized by chemical routes: A comparison between coprecipitation and sol-gel," *J. Alloys Compd.*, vol. 798, pp. 311–319, Aug. 2019, doi: 10.1016/j.jallcom.2019.05.170.

[53] K. G. Schell, E. C. Bucharsky, F. Lemke, and M. J. Hoffmann, "Effect of calcination conditions on lithium conductivity in $Li_{1.3}Ti_{1.7}Al_{0.3}(PO_4)_3$ prepared by sol-gel route," *Ionics (Kiel).*, vol. 23, no. 4, pp. 821–827, Apr. 2017, doi: 10.1007/s11581-016-1883-y.

[54] P. Bhanja, C. Senthil, A. K. Patra, M. Sasidharan, and A. Bhaumik, "NASICON type ordered mesoporous lithium-aluminum-titanium-phosphate as electrode materials for lithium-ion batteries," *Microporous Mesoporous Mater.*, vol. 240, pp. 57–64, Mar. 2017, doi: 10.1016/j.micromeso.2016.11.005.

[55] S. Duluard, A. Paillassa, L. Puech, P. Vinatier, V. Turq, P. Rozier, *et al.*, "Lithium conducting solid electrolyte $Li_{1.3}Al_{0.3}Ti_{1.7}(PO_4)_3$ obtained via solution chemistry," *J. Eur. Ceram. Soc.*, vol. 33, no. 6, pp. 1145–1153, Jun. 2013, doi: 10.1016/j.jeurceramsoc.2012.08.005.

[56] L. Huang, Z. Wen, M. Wu, X. Wu, Y. Liu, and X. Wang, "Electrochemical properties of $Li_{1.4}Al_{0.4}Ti_{1.6}(PO_4)_3$ synthesized by a co-precipitation method," *J. Power Sources*, vol. 196, no. 16, pp. 6943–6946, Aug. 2011, doi: 10.1016/j.jpowsour.2010.11.140.

[57] Y. Zhu, T. Wu, J. Sun, and M. Kotobuki, "Highly conductive lithium aluminum germanium phosphate solid electrolyte prepared by sol-gel method and hot-pressing," *Solid State Ionics*, vol. 350, p. 115320, Jul. 2020, doi: 10.1016/j.ssi.2020.115320.

[58] C. R. Mariappan, P. Kumar, A. Kumar, S. Indris, H. Ehrenberg, G. V. Prakash, *et al.*, "Ionic conduction and dielectric properties of yttrium doped $LiZr_2(PO_4)_3$ obtained by a Pechini-type polymerizable complex route," *Ceram. Int.*, vol. 44, no. 13, pp. 15509–15516, Sep. 2018, doi: 10.1016/j.ceramint.2018.05.211.

[59] G. B. Kunshina, I. V. Bocharova, and V. I. Ivanenko, "Effect of thermal treatment modes on ion-conducting properties of lithium-aluminum

  DOI: https://doi.org/10.60787/jcas.vol2no1.2|

titanophosphate," *Russ. J. Appl. Chem.*, vol. 90, no. 3, pp. 374–379, Mar. 2017, doi: 10.1134/S1070427217030089.

[60] H. Zhu and J. Liu, "Emerging applications of spark plasma sintering in all solid-state lithium-ion batteries and beyond," *J. Power Sources*, vol. 391, pp. 10–25, Jul. 2018, doi: 10.1016/j.jpowsour.2018.04.054.

[61] L. Hallopeau, D. Bregiroux, G. Rousse, D. Portehault, P. Stevens, G. Toussaint, *et al.*, "Microwave-assisted reactive sintering and lithium ion conductivity of $Li_{1.3}Al_{0.3}Ti_{1.7}(PO_4)_3$ solid electrolyte," *J. Power Sources*, vol. 378, pp. 48–52, Feb. 2018, doi: 10.1016/j.jpowsour.2017.12.021.

[62] X. Wei, J. Rechtin, and E. Olevsky, "The Fabrication of All-Solid-State Lithium-Ion Batteries via Spark Plasma Sintering," *Metals (Basel).*, vol. 7, no. 9, p. 372, Sep. 2017, doi: 10.3390/met7090372.

[63] J. Feng, H. Xia, M. O. Lai, and L. Lu, "NASICON-Structured $LiGe_2(PO_4)_3$ with Improved Cyclability for High-Performance Lithium Batteries," *J. Phys. Chem. C*, vol. 113, no. 47, pp. 20514–20520, Nov. 2009, doi: 10.1021/jp9085602.

[64] H. Aono, E. Sugimoto, Y. Sadaoka, N. Imanaka, and G. Adachi, "Electrical properties and sinterability for lithium germanium phosphate $Li_{1+x}M_xGe_{2-x}(PO_4)_3$, M=Al, Cr, Ga, Fe, Sc, and in systems," *Bull. Chem. Soc. Jpn.*, vol. 65, no. 8, pp. 2200–2204, 1992.

[65] Y. Liu, J. Chen, and J. Gao, "Preparation and chemical compatibility of lithium aluminum germanium phosphate solid electrolyte," *Solid State Ionics*, vol. 318, pp. 27–34, May 2018, doi: 10.1016/j.ssi.2017.10.016.

[66] M. Sugantha and U. V Varadaraju, "Ionic conductivity of Li^+ ion conductors $Li_2M^{3+}\ M^{4+}\ P_3O_{12}$," *Solid State Ionics*, vol. 95, no. 3–4, pp. 201–205, 1997, doi: 10.1016/S0167-2738(96)00565-6.

[67] A. Venkateswara Rao, V. Veeraiah, A. V. Prasada Rao, and B. Kishore Babu, "Effect of Fe^{3+} doping on the structure and conductivity of $LiTi_2(PO_4)_3$," *Res. Chem. Intermed.*, vol. 41, no. 4, pp. 2307–2315, Apr. 2015, doi: 10.1007/s11164-013-1348-0.

[68] R. Kahlaoui, K. Arbi, R. Jimenez, I. Sobrados, J. Sanz, and R. Ternane, "Influence of preparation temperature on ionic conductivity of titanium-defective $Li_{1+4x}Ti_{2-x}(PO_4)_3$ NASICON-type materials," *J. Mater. Sci.*, vol. 55, no. 20, pp. 8464–8476, Jul. 2020, doi: 10.1007/s10853-020-04463-3.

[69] A. Belous, G. Kolbasov, L. Kovalenko, E. Boldyrev, S. Kobylianska, and B. Liniova, "All solid-state battery based on ceramic oxide electrolytes with perovskite and NASICON structure," *J. Solid State Electrochem.*, vol. 22, no. 8, pp. 2315–2320, Aug. 2018, doi: 10.1007/s10008-018-3943-x.

[70] A. Venkateswara Rao, V. Veeraiah, A. V. Prasada Rao, B. Kishore Babu, and K. V. Kumar, "Influence of Zr^{4+} doping on structural, spectroscopic and conductivity studies of lithium titanium phosphate," *Ceram. Int.*, vol. 40, no. 9, pp. 13911–13916, Nov. 2014, doi: 10.1016/j.ceramint.2014.05.111.

[71] Z. Li and X. Zhao, "Influence of excess lithium and sintering on the conductivity of $Li_{1.3}Al_{0.3}Ti_{1.7}(PO_4)_3$," *Funct. Mater. Lett.*, vol. 12, no. 04, p. 1950047, Aug. 2019, doi: 10.1142/S1793604719500474.

[72] R. Kahlaoui, K. Arbi, R. Jimenez, I. Sobrados, J. Sanz, and R. Ternane, "Distribution and mobility of lithium in NASICON-type $Li_{1-x}Ti_{2-x}Nb_x(PO_4)_3$ ($0 \le x \le 0.5$) compounds," *Mater. Res. Bull.*, vol. 101, pp. 146–154, May 2018, doi: 10.1016/j.materresbull.2018.01.022.

[73] H. Aono, E. Sugimoto, Y. Sadaoka, N. Imanaka, and G. Adachi, "Electrical properties and crystal structure of solid electrolyte based on lithium hafnium phosphate $LiHf_2(PO_4)_3$," *Solid State Ionics*, vol. 62, no. 3–4, pp. 309–316, Aug. 1993, doi: 10.1016/0167-2738(93)90387-I.

[74] R. Kahlaoui, K. Arbi, I. Sobrados, R. Jimenez, J. Sanz, and R. Ternane, "Cation Miscibility and Lithium Mobility in NASICON $Li_{1+x}Ti_{2-x}Sc_x(PO_4)_3$ ($0 \le x \le 0.5$) Series: A Combined NMR and Impedance Study," *Inorg. Chem.*, vol. 56, no. 3, pp. 1216–1224, Feb. 2017, doi: 10.1021/acs.inorgchem.6b02274.

[75] A. Cassel, B. Fleutot, M. Courty, V. Viallet, and M. Morcrette, "Sol-gel synthesis and electrochemical properties extracted by phase inflection detection method of NASICON-type solid electrolytes $LiZr2(PO_4)_3$ and $Li_{1.2}Zr_{1.9}Ca_{0.1}(PO_4)_3$," *Solid State Ionics*, vol. 309, pp. 63–70, Oct. 2017, doi: 10.1016/j.ssi.2017.07.009.

[76] Y. Zhang, K. Chen, Y. Shen, Y. Lin, and C.-W. Nan, "Enhanced lithium-ion conductivity in a $LiZr_2(PO_4)_3$ solid electrolyte by Al doping," *Ceram. Int.*, vol. 43, pp. S598–S602, Aug. 2017, doi: 10.1016/j.ceramint.2017.05.198.

[77] B. E. Francisco, C. R. Stoldt, and J.-C. M'Peko, "Lithium-Ion Trapping from Local Structural Distortions in Sodium Super Ionic Conductor (NASICON) Electrolytes," *Chem. Mater.*, vol. 26, no. 16, pp. 4741–4749, Aug. 2014, doi: 10.1021/cm5013872.

[78] E. Yi, K. Yoon, H.-A. Jung, T. Nakayama, M. Ji, and H. Hwang, "Fabrication and electrochemical properties of $Li_{1.3}Al_{0.3}Ti_{1.7}(PO_4)_3$ solid electrolytes by sol-gel method," *Appl. Surf. Sci.*, vol. 473, pp. 622–626, Apr. 2019, doi: 10.1016/j.apsusc.2018.12.202.

[79] X. Xu, Z. Wen, X. Yang, and L. Chen, "Dense nanostructured solid electrolyte with high Li-ion conductivity by spark plasma sintering technique,"

  DOI: https://doi.org/10.60787/jcas.vol2no1.2|

Mater. Res. Bull., vol. 43, no. 8–9, pp. 2334–2341, Aug. 2008, doi: 10.1016/j.materresbull.2007.08.007.

[80] S. Breuer, D. Prutsch, Q. Ma, V. Epp, F. Preishuber-Pflügl, F. Tietz, *et al.*, "Separating bulk from grain boundary Li ion conductivity in the sol–gel prepared solid electrolyte $Li_{1.5}Al_{0.5}Ti_{1.5}(PO_4)_3$," *J. Mater. Chem. A*, vol. 3, no. 42, pp. 21343–21350, 2015, doi: 10.1039/C5TA06379E.

[81] P. Zhang, M. Matsui, A. Hirano, Y. Takeda, O. Yamamoto, and N. Imanishi, "Water-stable lithium ion conducting solid electrolyte of the $Li_{1.4}Al_{0.4}Ti_{1.6-x}Ge_x(PO_4)_3$ system (x=0–1.0) with NASICON-type structure," *Solid State Ionics*, vol. 253, pp. 175–180, Dec. 2013, doi: 10.1016/j.ssi.2013.09.022.

[82] V. Ramar, S. Kumar, S. R. Sivakkumar, and P. Balaya, "NASICON-type La^{3+}substituted $LiZr_2(PO_4)_3$ with improved ionic conductivity as solid electrolyte," *Electrochim. Acta*, vol. 271, pp. 120–126, May 2018, doi: 10.1016/j.electacta.2018.03.115.

[83] M. I. Kimpa, M. Z. H. Mayzan, F. Esa, J. A. Yabagi, M. M. Nmaya, and M. A. Agam, "Sol-Gel Synthesis and Electrical Characterization of $Li_{1+x}Al_xTi_{2-x}(PO_4)_3$ Solid Electrolytes," *J. Sci. Technol.*, vol. 9, no. 3, 2017.

[84] M. Perez-Estébanez, M. Peiteado, A. C. Caballero, F. J. Palomares, M. Nygren, and J. Isasi-Marín, "SPS driven lithium differential diffusion in NASICON-like structures," *Boletín la Soc. Española Cerámica y Vidr.*, vol. 55, no. 1, pp. 38–44, Jan. 2016, doi: 10.1016/j.bsecv.2015.11.005.

[85] C. Chang, Y. Il Lee, S. Hong, and H. Park, "Spark Plasma Sintering of $LiTi_2(PO_4)_3$ -Based Solid Electrolytes," *J. Am. Ceram. Soc.*, vol. 88, no. 7, pp. 1803–1807, Jul. 2005, doi: 10.1111/j.1551-2916.2005.00246.x.

[86] Y. Nikodimos, M. C. Tsai, L. H. Abrha, H. H. Weldeyohannis, S. F. Chiu, H. K. Bezabh, *et al.*, "Al–Sc dual-doped $LiGe_2(PO_4)_3$ – a NASICON-type solid electrolyte with improved ionic conductivity," *J. Mater. Chem. A*, vol. 8, no. 22, pp. 11302–11313, 2020, doi: 10.1039/D0TA00517G.

[87] H. R. Arjmandi and S. Grieshammer, "Defect formation and migration in Nasicon $Li_{1+x}Al_xTi_{2-x}(PO_4)_3$," *Phys.*

  DOI: https://doi.org/10.60787/jcas.vol2no1.2|